A Study on Nucleation Kinetics of Carbamazepine-Fumaric Acid Form B Cocrystal

Mohamad Zulhelmi Mohd Zawawi, Dr. Nornizar Anuar, Dr. Syarifah Abd Rahim, and Umi Rafiah Shukri,

Faculty of Chemical Engineering, Universiti Teknologi Mara

***Abstract*— Cocrystallization is a common technique selected by many reseachers in purpose to enhance pharmaceutical drugs properties and nucleation kinetics is one of the important parameter to perform cocrystallization. However, the nucleation kinetics for carbamazepine-fumaric acid form B cocrystal has not been studied. The purpose of this experiment is to study on nucleation kinetics of CBZ-FUM acid form B by using Nývlt approach. In this study, carbamazepine (CBZ) was selected as API and fumaric acid (FUM) was used as coformer in order to produce CBZ-FUM form B cocrystal. To ensure form B was produced, stoichiometric ratio of 1:2 of CBZ to FUM was used in this study. Metastable zone width (MSZW) was studied by manipulating the solution concentration in range from 0.0467 g/mL to 0.0512 g/mL. Besides that, the effect of cooling rate on MSZW also was studied by varying the cooling rate (0.10, 0.25, 0.50, and 0.75 ˚C/min). Based on results obtained, the MSZW was increased as cooling rate increases but concentration has insignificant effect on MSZW. The nucleation rate obtained was in range of 0.1325 to 1.3052. Cocrystal also was undergo characterization process by using FTIR microscopy and optical microscope. Based on FTIR results, cocrystal peaks was formed on above and below of peaks of pure component. Meanwhile, form B cocrystal that formed has needle-liked morphology.**

Keywords*— *Carbamazepine, fumaric acid, metastable zone widths, nucleation kinetics, polythermal method.

I. INTRODUCTION

Pharmaceutical drug is classified into several classes based on its pharmaceutical properties. Each classes had unique and different characteristics compared to other classes. For example, carbamazepine is pharmaceutical drug class II has low solubility and high permeability in biopharmaceutical system [1]. There are several techniques to enhance the pharmaceutical drug properties such as solid dispersion, micronization, emulsification and crystallization. Crystallization is a method that involves the separation of solid matter from liquid phase. Nowadays, cocrystallization method is commonly used by many researchers to increase bioavailability of pharmaceutical drug. It consists of two or more components, where one component is an active pharmaceutical ingredient (API) and another one is made up of coformer component [2]. Both components linked together by hydrogen bond without making or breaking the covalent bond [3].

Improving crystal properties can be achieved by investigating the crystallization thermodynamics such as solution supersaturation and metastable zone width (MSZW) [4]. Creation of new solid interfaces in solution only can be achieved at certain level of supersaturation. Meanwhile, MSZW measurement is important to characterize nucleation and for crystallization process evaluation.

MSZW is a region between supersolubility and solubility curve as shown in Fig. 1. Supersolubility and solubility curve also known as cloud and clear point curves respectively [5]. The width of metastable zone can be calculated by taking temperature difference between saturation and nucleation temperature. MSZW is consider as important parameter in order to calculate the nucleation kinetic for the process. Determination on MSZW can be experimentally determined by polythermal method. Polythermal method is an experiment where saturated solution is cooled down in constant rate until nucleation is occurred [6].

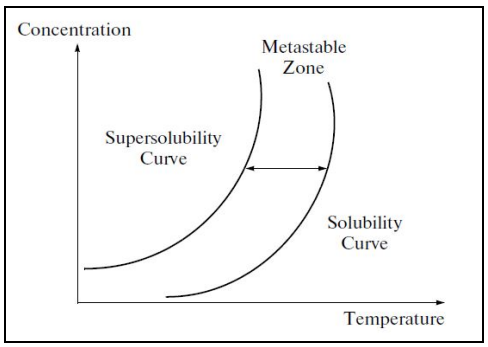

Fig. 1: Metastable zone width (MSZW) [3]

In order to estimate the nucleation rate of the process, Nývlt approach was utilized. According to Nývlt approach, the nucleation rate at the beginning is assumed correspond to supersaturation for limited time period [7]. The nucleation rate, J_n, can be determined using the following power law expression as a function of supersaturation Δc [5]

$$J = k'(\Delta c)^m \quad (1)$$

where k' is nucleation rate constant, Δc is the supersaturation or differences between concentration and solubility concentration of the solution (Δc = c - c*). The rate of supersaturation for cooling crystallization can be written as a function of cooling rate, R, as follow [4]:

$$\frac{d\Delta c}{dt} = R\frac{dc^*}{dT} \quad (2)$$

where dc*/dt is slope of the solubility curve at given saturation temperature. Upon nucleation, the relationship between supersaturation and MSZW by [5]:

$$\Delta c_{max} = \Delta T_{max}\frac{dc^*}{dT} \quad (3)$$

where MSZW can be expressed as [5]:

$$\Delta T_{max} = T^* - T_{nuc} \quad (4)$$

By using assumption when at the beginning, the nucleation rate is corresponds to supersaturation rate, the relationship between number of nuclei formed and mass of formed nuclei is given as [5]:

$$\frac{dM}{dt} = k'\alpha\rho_c r^3 \Delta c^m = k_n \Delta c^m \quad (5)$$

where k_n is the mass nucleation rate constant, M is the mass of formed nuclei and terms ρ_c and α are density of solute crystal and the volume shape factor, respectively.

Thus, by combining Eqs. (2), (4), and (5) will yields the following expression [5]:

$$k_n \Delta c^m = k_n \left[\left(\frac{dc^*}{dT} \right) \Delta T_{max} \right]^m = R \left(\frac{dc^*}{dT} \right) \varepsilon \quad (6)$$

where ε is conversion factor that consider the concentration changes due to formation of hydrates or solvates. This conversion factor can be formulated as follows [5]:

$$\varepsilon = \frac{R_h}{[1 - c(R_h - 1)]^2} \quad (7)$$

where R_h is known as ratio of molecular weight of hydrate to molecular weight of anhydrate and c is solution concentration in terms of mass of anhydrate per unit mass of solvates. Rearranging Eq. 6 and taking logarithm of both sides yield an expression as follows [5]:

$$\ln R = m[\ln(\Delta T_{max})] + \ln k_n + (m-1)\ln\left(\frac{dc^*}{dT} \right) \quad (8)$$

By rearranging Eq. 8 where ΔTmax is equivalent to MSZW yield an expression as follows:

$$\ln(MSZW) = \frac{1-m}{m}\ln\left(\frac{dc^*}{dT} \right) - \frac{1}{m}\ln k + \frac{1}{m}\ln R \quad (9)$$

The above equation can be plotted into a log plot of MSZW, ln (MSZW), versus the log plot of cooling rate, ln R, at given saturation temperature. This plot should result in straight line where the slope is representing the apparent nucleation order, m and mass nucleation rate constant, k_n, can be estimated from intercept.

Thus, the purpose of this paper is to study the nucleation kinetics of carbamazepine-fumaric acid from B cocrystal by utilizing Nývlt approach. The dissolution and cocrystallization diagram was employed for estimation of metastable zone (MSZW). Besides that, the morphology of CBZ-FUM form B cocrystal also was studied.

II. METHODOLOGY

A. Materials

The experimental work outlined was performed on carbamazepine (CBZ), fumaric acid (FUM), and ethanol as a solvent from HmbG Chemical with 99% purity.

B. Solution Concentration and Cooling Rate

This MSZW experiments were done in batch jacketed reactor with programmable refrigerated bath based on desired heating or cooling rate. The cooling rates were varied from 0.10 ˚C/min, 0.25 ˚C/min, 0.50 ˚C/min, and 0.75 ˚C/min. The reactor was equipped with glass stirrer to ensure uniform mixing of solution. The agitation speed for stirrer is constant at 800 rpm during heating stage and was reduced to 50 rpm during cooling stage. Meanwhile, for solution concentration during cooling stage for each cooling rate was varied from 0.0456 g/mL, 0.0476 g/mL, 0.0488 g/mL, 0.0500 g/mL, and 0.0512 g/mL. Meanwhile, for heating process, it varied from 0.0163 g/mL, 0.0167 g/mL, 0.0171 g/mL, 0.0188 g/mL, and 0.0194 g/mL.

C. Crystal Sampling

Cocrystallization of CBZ-FUM was prepared by mixing together both CBZ and FUM in powder form. In order to obtain CBZ-FUM form B cocrystal, molar ratio of 1:2 for CBZ to FUM was utilized. This compound was inserted into the reactor and 100 mL of ethanol was added in order for dissolving the compound. The solution was heated to target temperature which is 50 ˚C about 15 minutes. Then, it was allowed to heat continuously about one hour at target temperature or minimum 15 ˚C above the saturation temperature for ensure complete dissolution of the solution.

Next, solution was undergo cooling stage where first nucleation or creation of new solid in solution occurred. At this stage, solution was cooled to 20 ˚C according to desired cooling rate. The temperature where first nucleation occurs was recorder and marked as nucleation temperature (T_{crys}). Cocrystal of CBZ-FUM started to appear inside the reactor vessel. It was allowed to cool continuously about 2 hours at 20 ˚C for extended crystal growth.

For dissolution-crystallization curve determination, crystal formed in the reactor was filtered and dried until no changes on mass of cocrystal recorded. The cocrystal was weighted and dissolved with 100 mL of fresh ethanol inside the reactor. The cocrystal was heated to target temperature based on desired heating rate. Temperature where last cocrystal is dissolved was recorder and marked as dissolution temperature (T_{diss}). Both nucleation and dissolution temperature was plotted for each concentration and cooling rate for estimated the MSZW.

D. Crystal Characterization

For crystal characterization, cocrystal was characterized by using Fourier transform infrared (FTIR) microscopy and optical microscope. In characterization of CBZ-FUM cocrystal, FTIR microscopy (Thermo Nicolet) was used to study the interaction of OH-bonds among the molecules. This FTIR microscopy was operated at range of wave numbers of 500 to 4000 cm^{-1}. Furthermore, this microscopy was conducted 10 scans on samples to obtain average pattern for detected functional group. Before sample of CBZ-FUM cocrystal formed was placed on the plate, the plate was wiped with acetone to ensure that impurities on the plate are removed. Then, dried cocrystal sample was located on the plate and characterization process by using FTIR microscopy was conducted. The FTIR result for CBZ-FUM form B cocrystal was compared to FTIR result for pure CBZ and pure FUM.

To study the morphology of cocrystal formed, optical microscope was used to observe the morphology of CBZ-FUM form B cocrystal. Optical microscope (Olympus BX41) was used and it was equipped with analySIS software. This microscope was able to magnify the cocrystal image into 4 times (4x), 10 times (10x), 20 times (20x) and 40 times (40x). The scale was provided according to magnification of this microscope was 500 µm, 200 µm, 100 µm, and 50 µm, respectively. The cocrystal was recovered from the solution and was observed under the microscope.

III. RESULTS AND DISCUSSION

A. Dissolution and Crystallization Diagram

The dissolution and crystallization curve was made up of a set of data of dissolution temperature (T_{diss}) and crystallization temperature (T_{crys}). Due to different concentration for T_{crys} and T_{diss}, and limitation for MSZW estimation, T_{diss} was obtained by extrapolated the power trendline of dissolution curve as shown in Fig. 2. Based on result obtained from the MSZW graph, it can be concluded that dissolution temperature (T_{diss}) for each of cooling rate has slightly constant and similar pattern. This result support that solution heating rate does not influence the dissociation behavior of cocrystal in contrast to crystallization on-set where this low nucleation rate material affects a greater undercooling for faster cooling rate [8].

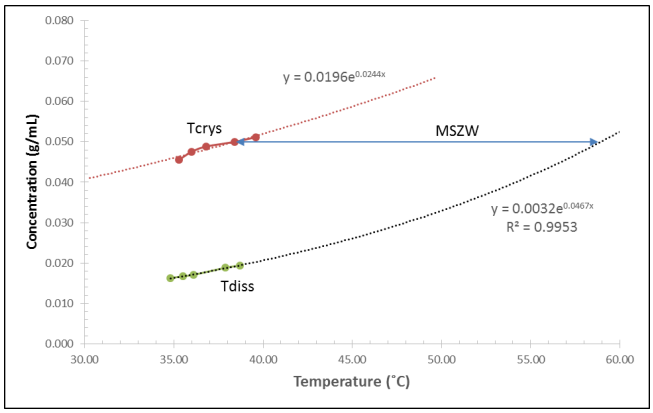

Fig. 2: Extrapolated T_{diss} with corresponding MSZW for 0.75 °C/min

B. *Metastable Zone Width (MSZW)*

Thus, MSZW was estimated based on dissolution and crystallization diagram that was plotted for each cooling rate. Dissolution temperature, crystallization temperature and MSZW were summarized in Table 1. Based on result in Table 1, it can be concluded that the width of metastable zone was increased as cooling rate increased. For crystallization process in industry, they are preferred process that has larger MSZW and high rate of reaction. The wider of MSZW is able to allow better control on product size and nucleation is easier to form when nucleation rate is high [9]. The extrapolated method was utilized in order to get T_{diss} and T_{crys} at cooling rate approximately to 0 °C/min as shown in Fig. 3.

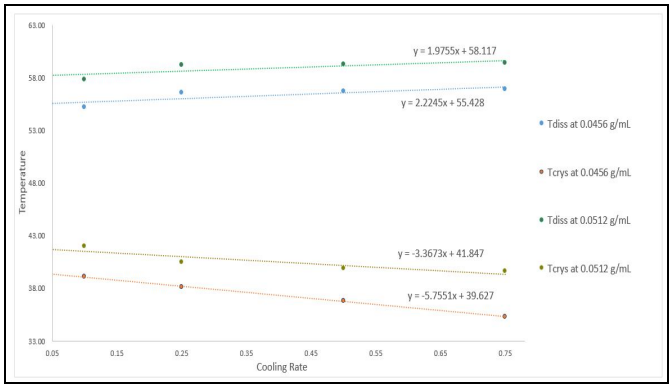

Fig. 3: Extrapolated for T_{crys} and T_{diss} with corresponding to 0°C/min

Table 1: MSZW estimated from dissolution and crystallization diagram and T_{diss} and T_{crys} from extrapolated curve at 0°C/min

0.0456 g/mL					
Cooling rate, R (°C/min)	≈0	0.10	0.25	0.50	0.75
T_{diss} (°C)	55.43	55.18	56.53	56.67	56.89
T_{crys} (°C)	39.63	39.10	38.10	36.80	35.30
MSZW	15.80	16.08	18.43	19.87	21.59
0.0476 g/mL					
Cooling rate, R (°C/min)	≈0	0.10	0.25	0.50	0.75
T_{diss} (°C)	56.43	56.16	57.51	57.63	57.81
T_{crys} (°C)	41.08	40.80	38.80	37.60	36.00
MSZW	15.35	15.36	18.71	20.03	21.81
0.488 g/mL					
Cooling rate, R (°C/min)	≈0	0.10	0.25	0.50	0.75
T_{diss} (°C)	57.01	56.72	58.09	58.19	58.34
T_{crys} (°C)	41.49	41.40	39.20	37.90	36.80
MSZW	15.52	15.32	18.89	20.29	21.54
0.0500 g/mL					
Cooling rate, R (°C/min)	≈0	0.10	0.25	0.50	0.75
T_{diss} (°C)	57.56	57.27	58.64	58.73	58.86
T_{crys} (°C)	41.70	41.70	40.10	38.60	38.40
MSZW	15.86	15.57	18.54	20.13	20.46
0.0512 g/mL					
Cooling rate, R (°C/min)	≈0	0.10	0.25	0.50	0.75
T_{diss} (°C)	58.12	57.81	59.19	59.26	59.37
T_{crys} (°C)	41.85	42.00	40.50	39.90	39.60
MSZW	16.27	15.81	18.69	19.36	19.77

C. *Nucleation Kinetics*

To study the nucleation kinetics of CBZ-FUM form B cocrystal, Nývlt approach was utilized. nucleation constant, k and nucleation Log plots of MSZW versus cooling rate as shown in Fig. 4 was plotted and slope and intercept of the graph has being utilized to estimate the nucleation order, m, rate, J.

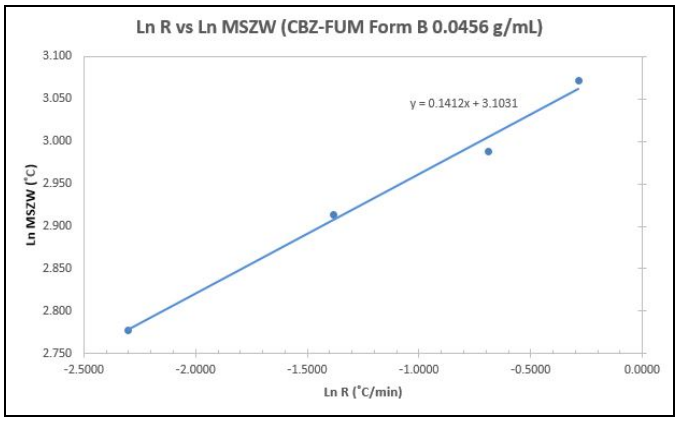

Fig. 4: Procedure to determine the value of nucleation order, m and nucleation constant, k

Based on result in graph, it can be concluded that a linear relationship exists between MSZW and cooling rate parameter. The nucleation parameter is being utilized by using slope and intercept of a power trendline of these points [10]. By comparing the slope and intercept to Eq. 9, the value for nucleation order, m, and nucleation rate constant, k_n, was obtained as shown in Table 2(a-e).

Table 2(a): Nucleation parameter at concentration 0.0456 g/mL

Cooling Rate (°C/min)	k_n	m
0.10	3.0531 E-11	7.0822
0.25	4.2230 E-11	
0.50	5.2917 E-11	
0.75	4.8455 E-11	

Table 2(b): Nucleation parameter at concentration 0.0476 g/mL

Cooling Rate (°C/min)	k_n	m
0.10	1.0536 E-09	5.9701
0.25	1.1242 E-09	
0.50	1.5409 E-09	

0.75	1.4132 E-09	

Table 2(c): Nucleation parameter at concentration 0.0488 g/mL

Cooling Rate (˚C/min)	k_n	m
0.10	7.7096 E-10	6.0314
0.25	7.6764 E-10	
0.50	1.0128 E-09	
0.75	1.0390 E-09	

Table 2(d): Nucleation parameter at concentration 0.0500 g/mL

Cooling Rate (˚C/min)	k_n	m
0.10	1.3901 E-11	7.2098
0.25	1.5289 E-11	
0.50	1.6931 E-11	
0.75	2.1108 E-11	

Table 2(e): Nucleation parameter at concentration 0.0512 g/mL

Cooling Rate (˚C/min)	k_n	m
0.10	2.1517 E-14	9.1158
0.25	2.1118 E-14	
0.50	3.0055 E-14	
0.75	3.2252 E-14	

Thus, by considering nucleation constant and nucleation order from Table 2, the nucleation rate can be calculated by substituting into Eq. 1 as shown in Table 3.

Table 3: Nucleation rate

Cooling rate (˚C/min)	0.10	0.25	0.50	0.75
0.0456 g/mL	0.1345	0.3696	0.7548	1.2421
0.0476 g/mL	0.1754	0.3522	0.6948	0.9521
0.0488 g/mL	0.1763	0.3431	0.6360	0.9238
0.0500 g/mL	0.1577	0.4011	0.6452	1.1360
0.0512 g/mL	0.1325	0.3933	0.8612	1.3052

Based on results in Table 2, nucleation order shows that range from 5.9701 to 9.1158. It shows that the nucleation was increased as concentration of nucleation increases. Each concentration solution has same nucleation order since the value was obtained from slope of the graph. The nucleation rate does not affect the nucleation order at same solution concentration. Meanwhile for nucleation constant, the values were consistent for concentration of 0.0456, 0.0476, 0.0500, and 0.0512 g/mL. However, there is inconsistent values was recorded for concentration at 0.0488 g/mL. For nucleation rate, nucleation order and nucleation constant was utilized by using Eq. 1. Based on nucleation rate that was represented in Table 3, the value was in range from 0.1325 to 1.3052. The result showed that the nucleation rate was increased as cooling rate increases. Thus, it can be concluded that the best cooling rate is 0.75 ˚C/min and the concentration of solution is 0.0512 g/mL.

D. Optical Microscope

Morphology of CBZ-FUM form B cocrystal was studied by using optical microscope and was compared with morphology of pure CBZ and FUM crystal. Based on microscope image in Fig.5, mostly cocrystal that formed have needle-liked morphology. Different cooling rate show no significant differences in crystal morphology. In addition, small cocrystal was formed due to slow process growth of cocrystal. The introduction of stirrer was caused the movement of solution such as stirring and shaking. Thus, it was induced the nucleation and small crystals was grown resulted small co-crystal size [11].

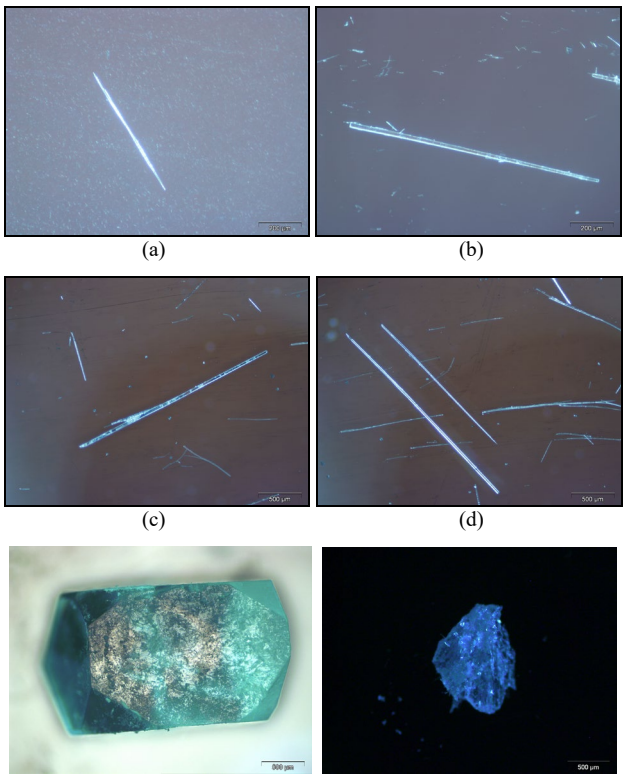

(a) (b) (c) (d) (e) (f)

Fig. 5: CBZ-FUM form B cocrystal morphology for (a) cooling rate at 0.10 ˚C/min, (b) 0.25 ˚C/min, (c) 0.50 ˚C/min, (d) 0.75 ˚C/min, (e) pure CBZ and (f) fumaric acid

E. Fourier Transform Infrared (FTIR) Microscopy

The cocrystal of CBZ-FUM form B was analyzed by using FTIR microscopy to detect the present of functional group and was compared with IR spectrum for pure CBZ and pure FUM as shown in Fig. 6, Fig. 7, Fig. 8, and Fig. 9.

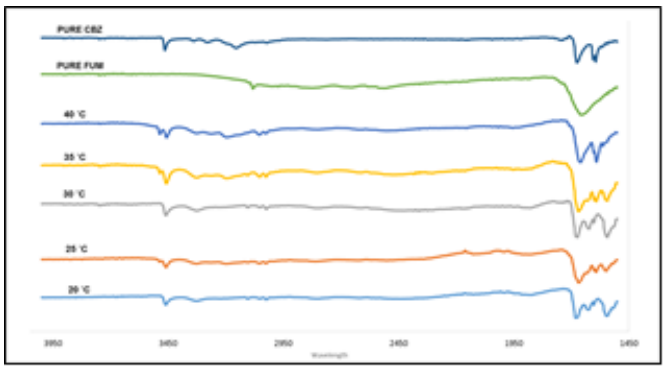

Fig. 5: FTIR result for 0.10 ˚C/min

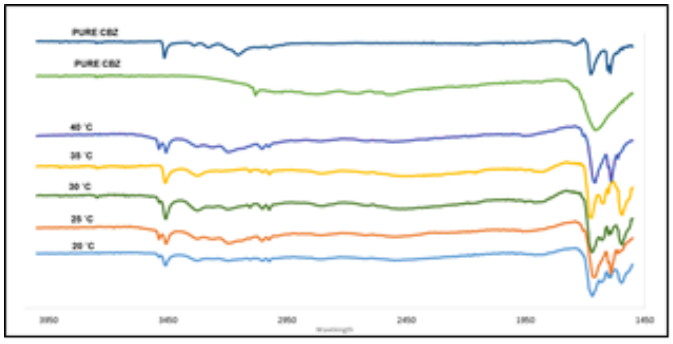

Fig. 6: FTIR result for 0.25 ˚C/min

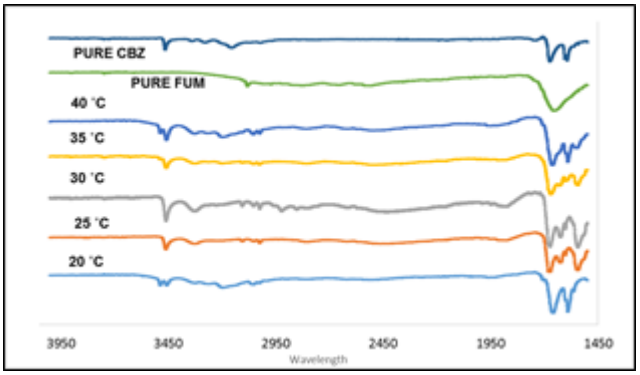

Fig. 7: FTIR result for 0.50 ˚C/min

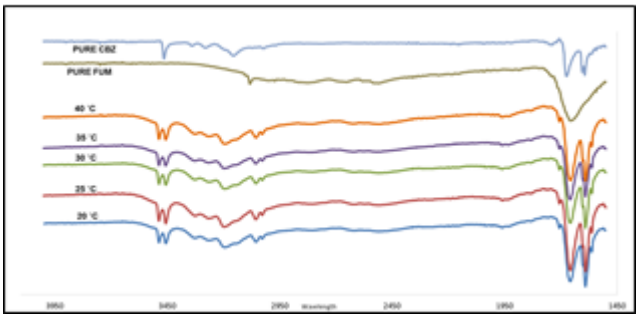
Fig. 8: FTIR result for 0.75 ˚C/min

The characteristic of CBZ and FUM peaks was studied by using FTIR microscopy. It was showed that the CBZ peaks were observed at 3464, 1674, 1604, and 1593 cm^{-1} [12]. Meanwhile, for co-former FUM, the peaks were observed at 3081 cm^{-1} and 1657 cm^{-1}. Both CBZ and FUM peaks that were obtained had shown similar result with reference [13]. The peak profiles of CBZ-FUM form B cocrystal was observed higher or lower compared to pure component. The formation of CBZ-FUM co-crystal can be confirmed by observing the significant changing on wavelength such as shifting of peak represent amide and carboxylic acid functional group [14]. For CBZ-FUM form B, the peaks for amides have shifted to 3460 cm^{-1}, 1680 cm^{-1} and 1600 cm^{-1}. This peak represents N-H stretch, C=O and N-H bend, respectively. Otherwise, for carboxylic acid peaks was observed at 3052 cm^{-1} and 1673 cm^{-1}. This peaks were represented the (O-H stretch) and (C=O) [15].

IV. Conclusion

The formation of CBZ-FUM form B cocrystal was investigated by using polythermal method. In order to ensure that form B cocrystal is formed instead of other forms, 1:2 molar ratio of CBZ to FUM was used in this study. The main purpose of this study to determine the nucleation kinetics of CBZ-FUM form B cocrystal was investigated. Based on nucleation rate that was calculated, it shows that the nucleation kinetic for each cooling rate has quite similar values. For MSZW study, the width of metastable zone was increased as cooling rate increases. Based on FTIR result, it proved that cocrystal was formed where significant shifting of peaks were observed in IR spectrum for form B cocrystals. The shifting peak that was observed represents the amide and carboxylic acid group. For study on crystal morphology, optical microscope was used to observe the morphology of CBZ-FUM form B cocrystal. Based on image results, form B cocrystal was formed have needle-like shape morphology. There is no significant effect of cooling rate on morphology of cocrystal that was recorded. In particular, some barriers that effect the result were detected such as inaccurate data collection for nucleation temperature due to observation by using naked eyes. Evaporation of solvent (ethanol) also leads to change in concentration and it need to be controlled.

Acknowledgment

The authors would like to thanks Faculty of Chemical Engineering, UiTM for facilities provided for this research. This research is part of grant 600-IRMI/MyRA/5/3/BESTARI/023/2017. This research project was prepared as a fulfillment for degree of Bachelor in Chemical Engineering and Process.

References

[1] Limwikrant, W., Nagai, A., Hagiwara, Y., Higashi, K., Yamamoto, K., & Moribe, K. (2012). Formation Mechanism of a New Carbamazepine/Malonic Acid Cocrystal Polymorph. *International Journal of Pharmaceutics,* 431, 237-240.

[2] Mundhe, A. V., Fuloria, N. K., & Biyani, K. R. (2013). Cocrystallization: An Alternative Approach for Solid Modification. *Journal of Drug Delivery & Therapeutics*, *3*(4), 166–172.

[3] Nanjwade, V. K., Manvi, F. V., Ali, S. M., Nanjwade, M. B. K., & Maste, M. M. (2011). New Trends in the Cocrystallization of Active Pharmaceutical Ingredient. *Journal of Applied Pharmaceutical Science,* 01(08), 1-5.

[4] Zeng, G., Li, H., Huang, S., Wang, X., & Chen, J. (2013). Determination of Metastable Zone Width and the Primary Nucleation Kinetics of Sodium Sulfate. *Theoretical Foundations of Chemical Engineering*, 49(6), 869-876.

[5] Mitchell, N. A., & Frawley, P. J. (2010). Nucleation Kinetics of Paracetamol-Ethanol Solutions from Metastable Zone Widths. *Journal of Crystal Growth*, *312*, 2740–2746.

[6] Gagnière, E., Mangin, D., Puel, F., Rivoire, A., Monnier, O., Garcia, E., & Klein, J. P. (2009). Formation of co-crystal: Kinetic and Thermodynamic Aspects. *Journal of Crystal Growth*, *311*, 2689–2695.

[7] Corzo, D. C. M., Borissova, A., Hammond, R. B., Kashchiev, D., Roberts, K. J., Lewtas, K., & More, I. (2013). Nucleation Mechanism and Kinetics from the Analysis of Polythermal Crystallisation Data: Methyl Stearate from Kerosene Solutions. *CrystEngComm*, *16*(6), 974–991.

[8] Kashchiev, D., Hammond, A. B., & Roberts, K. J. (2010). Effect of Cooling Rate on the Critical Undercooling for Crystallization. *Journal of Crystal Growth*, 312, 698-704.

[9] Anuar, N., Daud, W. R. W., Roberts, K. J., Kamarudin, S. T., & Tasirin, S. M. (2009). An Examination of the Solution Chemistry, Nucleation Kinetics, Crystal Morphology, and Polymorphic Behaviour of Aqueous phase Batch Crystallized L-Isoleucine at the 250 mL Scale Size. *Crystal Growth and Design*, 9(6), 2853-2862.

[10] Sangwal, K. (2010). On the Interpretation of Metastable Zone Width in anti-solvent Crystallization. *Cryst. Res. Technol.*, 45(9), 909-919.

[11] Rahim, S. A., Rahman, F. A., Nasir, E. N. E. M., & Ramle, N. A. (2015). Carbamazepine Co-crystal Screening with Dicarboxylic Acids Co-Crystal Formers. *International Journal of Environmental, Chemical, Ecological, Geological and Geophysical Engineering*, *9*(5), 442–445.

[12] Caliandro, R., Di Profio, G., & Nicolotti, O. (2013). Multivariate Analysis of Quaternary Carbamazepine–Saccharin Mixtures by X-ray Diffraction and Infrared Spectroscopy. *Journal of Pharmaceutical and Biomedical Analysis*, *78*(79), 269–279.

[13] Rahman, F. A., Rahim, S. A., Tan, C. C., Low, S. H., & Ramle, N. A. (2017). Carbamazepine-Fumaric Acid and Carbamazepine-Succinic Acid Co-crystal Screening Using Solution Based Method. *International Journal of Chemical Engineering and Applications*, 8(2), 136-140.

[14] Sevukarajan, M., Thanuja, B., Sodanapalli, R., & Nair, R. (2011). Synthesis and Characterization of a Pharmaceutical Sciences and Research. *Journal of Pharmaceutical Sciences and Research*, 3(6), 1288-1293.

[15] Du, Y., Fang, H. X., Zhang, Q., Zhang, H. L., and Hong, Z. (2016). Spectroscopic Investigation on Cocrystal Formation between Adenine and Fumaric Acid based on Infrared and Raman Techniques. *Molecular and Biomolecular Spectroscopy*, 153, 580-585.